DOI: 10.1002/ejoc.200600935

Visible-Light Photoresponsivity of a 4-(Dimethylamino)azobenzene Unit Incorporated into Single-Stranded DNA: Demonstration of a Large Spectral Change Accompanying Isomerization in DMSO and Detection of Rapid (*Z*)-to-(*E*) Isomerization in Aqueous Solution

Takashi Kamei,[a] Masabumi Kudo,[b] Haruhisa Akiyama,[b] Momoyo Wada,[b] Jun'ichi Nagasawa,[b] Masahiro Funahashi,[b] Nobuyuki Tamaoki,[b] and Taro Q. P. Uyeda*[a]

Keywords: Photoresponsivity / Oligonucleotides / 4-(Dimethylamino)azobenzene / (*E*)/(*Z*) isomerization / DNA nanodevices

We demonstrate significant visible-light photoresponsivity in a synthesized oligonucleotide containing a built-in pseudonucleotide possessing a 4-(dimethylamino)azobenzene (4-DMAzo) side chain. In dry DMSO as solvent, two clearly distinguishable spectra corresponding to the (*E*) and (Z) forms of the 4-DMAzo moiety tethered to the oligonucleotide were recorded with a conventional spectrophotometer before and after irradiation with 420 nm wavelength light, which induced (*E*)-to-(*Z*) isomerization. In addition, (Z)-to-(*E*) isomerization was accelerated by irradiation with either visible (λ = 550 nm) or UV (λ = 350 nm) light, demonstrating reversible photoresponsivity of the pseudo-oligonucleotide. In aqueous solutions the (Z)-to-(*E*) thermal isomerization of the photoresponsive pseudo-oligonucleotide was very rapid and was only detectable by laser flash photolysis.

Introduction

Azobenzene, a photochromic system, is widely used for syntheses of organic molecular devices that will undergo conformational changes by (*E*)/(*Z*) isomerization.[1–4] Synthetic oligonucleotides conjugated with azobenzene moieties[5,6] are promising examples of photoregulatable molecular devices. Asanuma et al. demonstrated reversible photoinduced isomerization of an azobenzene moiety incorporated in the form of an oligonucleotide side chain on irradiation with UV light ($300 < \lambda < 400$ nm) followed by visible light ($\lambda > 400$ nm), to induce (*E*)-to-(*Z*) and (*Z*)-to-(*E*) isomerization, respectively.[6] These authors further demonstrated that hybridization of the pseudo-oligonucleotide with a complementary oligonucleotide is destabilized by UV-induced structural changes in the azobenzene moiety,[7] and introduced a prototype DNA device in which an intramolecular hairpin structure could be opened by irradiation with UV light.[8] Oligonucleotides bearing tethered azobenzene derivatives with optical properties different from those of the parent azobenzene should permit more sophisticated photoregulation triggered by light of different wavelengths. As one example, tethering of oligonucleotides to two different azo-based photoresponsive moieties that could be induced to undergo (*E*)-to-(*Z*) and (*Z*)-to-(*E*) photoconversions independently of one another should allow four metastable conformations of the device, enabling site-selective or multi-step regulation of hybridization in DNA devices.

In this regard, it would be useful to develop oligonucleotides incorporating tethered azo-based photoresponsive components that would undergo reversible conformational changes in response to visible-light irradiation. Synthetic oligonucleotides conjugated with methyl red [4′-carboxy-4-(dimethylamino)azobenzene][9–12] have been shown to absorb visible light, and it has been suggested that methyl red conjugated oligonucleotides could be useful as DNA beacons thanks to their unique H-aggregation and stacking properties. When these oligonucleotides were irradiated with visible light in aqueous solution, however, no photoresponsivity of the oligonucleotides could be detected with a conventional spectrophotometer,[11,13] so little is currently known about the visible-light photoresponsivity of oligonucleotides incorporating tethered azobenzene derivatives with a dimethylamino group at the 4′-position, either in aqueous or in organic solutions.

In the work reported here we studied the physicochemical properties of a photoresponsive oligonucleotide incor-

[a] Research Institute for Cell Engineering, National Institute of Advanced Industrial Science and Technology (AIST), Higashi 1-1-1, Tsukuba, Ibaraki 305-8562, Japan
Fax: +81-29-861-3049
E-mail: t-uyeda@aist.go.jp
[b] Nanotechnology Research Institute, National Institute of Advanced Industrial Science and Technololgy (AIST), Higashi 1-1-1, Tsukuba, Ibaraki 305-8565, Japan

porating a 4-DMAzo unit upon visible-light irradiation (λ = 420 nm). In well dried DMSO as solvent, two different spectra representing the (*Z*) and (*E*) forms of 4-DMAzo tethered to the synthesized oligonucleotide were recorded with a conventional spectrophotometer. Furthermore, photoinduced reversible isomerization was demonstrated upon irradiation with light of different wavelengths (550 or 350 nm). In aqueous solution, though, the (*Z*)-to-(*E*) thermal isomerization was so rapid that it was detectable only by a flash photolysis technique.

Results and Discussion

Synthesis of Phosphoramidite Monomer 5

Prior to preparation of the photoresponsive oligonucleotides, a phosphoramidite monomer bearing a 4-DMAzo moiety was synthesized as shown in Scheme 1. Firstly, *N*,*N*-dimethyl-*p*-nitrosoaniline (**1**) was treated with *p*-phenylenediamine to form 4′-amino-4-DMAzo (**2**).[14] Then, in a manner similar to that described previously,[6,15] **2** and 2,2-bis(hydroxymethyl)propionic acid were condensed with elimination of water by use of dicyclohexylcarbodiimide and 1-hydroxybenzotriazole to form **3**. One of the two hydroxy groups in **3** was then protected by treatment with 4,4′-dimethoxytrityl chloride in the presence of 4-(dimethylamino)pyridine to form **4**, and finally, phosphitylation of **4** was performed with 2-cyanoethyl *N*,*N*,*N*′,*N*′-tetraisopropylphosphorodiamidite in the presence of 1*H*-tetrazole to form **5**, which was used for the synthesis of a photoresponsive oligonucleotide.

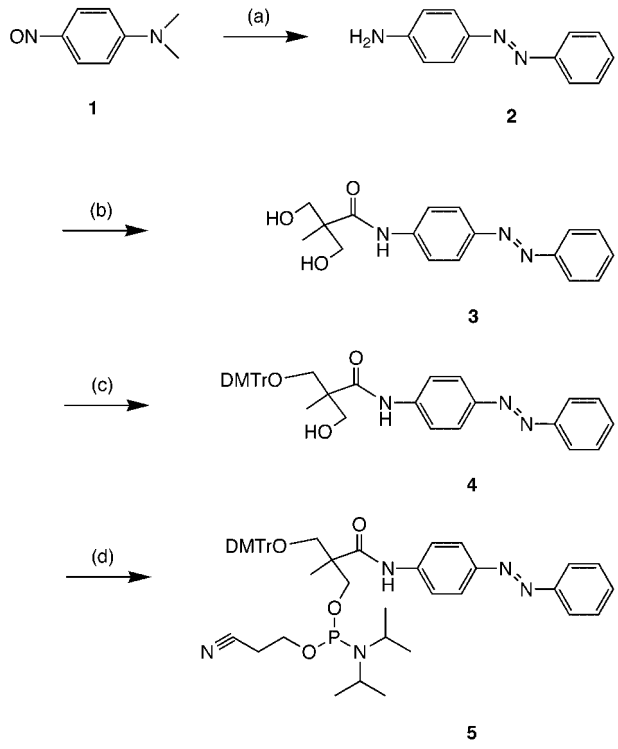

Scheme 1. Synthetic pathway for the phosphoramidite monomer **5**. (a) *p*-Phenylenediamine, glacial acetic acid, benzene, 42% yield. (b) 2,2-Bis(hydroxymethyl)propionic acid, 1-hydroxybenzotriazole, dicyclohexylcarbodiimide, DMF, 27% yield. (c) 4,4′-Dimethoxytrityl chloride (DMTr), 4-(dimethylamino)pyridine, pyridine, CH_2Cl_2, 53% yield. (d) 2-Cyanoethyl *N*,*N*,*N*′,*N*′-tetraisopropylphosphorodiamidite, 1*H*-tetrazole, acetonitrile, 36% yield.

Synthesis and HPLC Purification of Photoresponsive Pseudo-Oligonucleotides with 4-DMAzo Side Chains (6)

An oligonucleotide containing a built-in pseudo-nucleotide possessing a 4-DMAzo side chain (5′-AAAXAAAA-3′, where A is an adenosine residue and X is the residue bearing 4-DMAzo; Scheme 2) was prepared with an automated DNA synthesizer by use of **5**. The resultant pseudo-oligonucleotide **6** was purified by reversed-phase HPLC, and two major peaks were observed, indicating the existence of two stereoisomers of **6**,[6,16] both of which contained the thermally stable (*E*) form of 4-DMAzo. These two peaks were isolated and analyzed separately by MALDI-TOF mass spectrometry. The observed molecular masses of both compounds were 2549 ± 1, consistent with the calculated mass of [5′-AAAXAAAA-3′ + H^+] (2549).

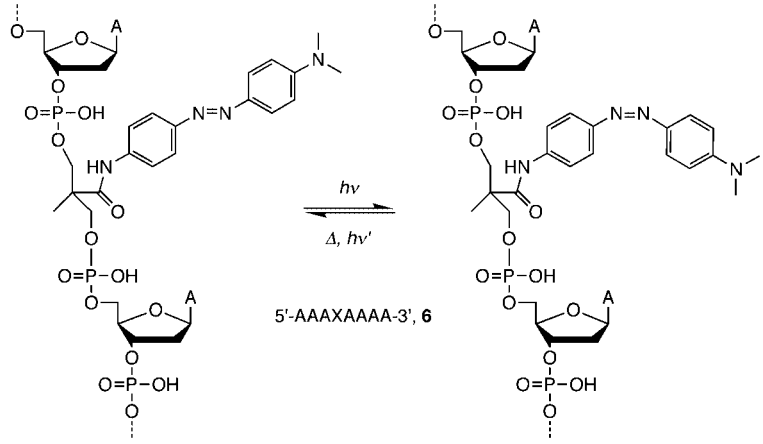

Scheme 2. Photoresponsive oligonucleotide **6** containing a built-in pseudonucleotide with a 4-DMAzo side chain. Reversible (*E*) (left)/(*Z*) (right) isomerization of the 4-DMAzo moiety (residue X) in **6**.

The two fractions from the reversed-phase HPLC were then freeze-dried under vacuum and stored. We used the fraction with the longer retention time in the experiments described below, although the other fraction behaved similarly with regard to photoresponsivity in a preliminary experiment (see Exp. Sect.).

Spectral Profiles of 6 and 4-DMAzo Derivatives

Figure 1 (a) shows spectra of the synthesized pseudo-oligonucleotide tethered to the (*E*) form of 4-DMAzo (**6**) in DMSO (solid line) and in water containing ammonium formate (50 mM, dotted line) before irradiation with visible light. Two major peaks were observed in each spectrum: one at ca. 260 nm and the other either at 426 nm (in DMSO) or at 462 nm (in aqueous solution). These peaks in the visible region were absent from the spectra of pure oligonucleotide solutions, indicating that they reflect absorption by the tethered 4-DMAzo in **6**. Hereafter, when we refer to "λ_{max}" for the pseudo-oligonucleotide, we are referring to the λ_{max} value for the 4-DMAzo moiety in the visible region. Table 1 summarizes the values of λ_{max} and half-bandwidth at the π–π* band for 4-DMAzo, the two derivatives of 4-DMAzo (4′-amino-4-DMAzo and 4′-acetoamide-4-DMAzo) (Scheme 3; **7**, **2**, and **8**, respectively), and **6** in organic and aqueous solutions before visible-light irradiation.

All compounds (**2**, **6**, **7**, and **8**) were soluble in DMSO, allowing comparison of the spectral properties of **6** [Figure 1 (b)] with those of the 4-DMAzo derivatives **7**, **2**, and **8** [Figure 1 (c–e), respectively]. The spectral profile and characteristic values (λ_{max} and half-bandwidth) for **6** (428 nm and 5381 cm^{-1}) in DMSO were very similar to those of **8** (426 nm and 5270 cm^{-1}) [gray solid lines in Figure 1 (b) and (e), respectively; Table 1], except for the absorption due to the oligonucleotide bases of **6** in the UV region. This suggests that the optical properties of **6** in the visible-light region are similar to those of **8**. The profile of **2** at the π–π* band is clearly different from those of **6**, **7**, and **8** [gray solid lines in Figure 1 (b–e)], with the large bathchromic shift (λ_{max} = 449 nm, 25 nm larger than that of **7**; Table 1) caused by the amino group at the 4′-position acting as an auxochrome. Unlike the amino group in **2**, the amide bonds in **6** and **8** linking the DMAzo moiety either to DNA (**6**) or to a methyl group (**8**) did not have large chromic effects on the π–π* band in the absorption spectra of the (*E*) form of 4-DMAzo.

Table 1. λ_{max} (nm) and half-bandwidth (cm^{-1}) values for the 4-DMAzo derivatives (**2**, **7**, **8**) and the photoresponsive oligonucleotide **6** in cyclohexane, DMSO, and water containing ammonium formate (50 mM). The spectra of compounds **2**, **6**, **7**, and **8** in DMSO and of **6** in the aqueous solution are shown in Figure 1. The spectra in cyclohexane are not shown.

Compound	Solvent		
	Cyclohexane	DMSO	Water
7	399 (4137)	424 (5129)	insoluble
2	403 (4870)	449 (5432)	insoluble
8	409 (4826)	428 (5381)	insoluble
6	insoluble	426 (5270)	462 (6093)

The solvent effects on the spectra of **6** and on the 4-DMAzo derivatives (**2**, **7**, and **8**) are as follows. In DMSO, which is more polar than cyclohexane, the λ_{max} values for 4-DMAzo and its derivatives were shifted to longer wavelengths than were seen in cyclohexane, accompanied by widening of the half-bandwidths by 550–1000 cm^{-1} (Table 1). The redshift of λ_{max} with increasing polarity of the solvent is consistent with an earlier result obtained with 4-(diethylamino)azobenzene.[17] In addition, although 4-DMAzo is insoluble in water, a redshift in the λ_{max} value for 4-DMAzo was observed in an organic/water co-solvent mixture.[18] The even larger redshift for the λ_{max} value of **6** in aqueous solution, accompanied by widening of the half-bandwidth (from 5270 cm^{-1} in DMSO to 6093 cm^{-1} in the aqueous solution, Table 1), is also consistent with the idea that larger redshifts are associated with higher solvent polarity.[17]

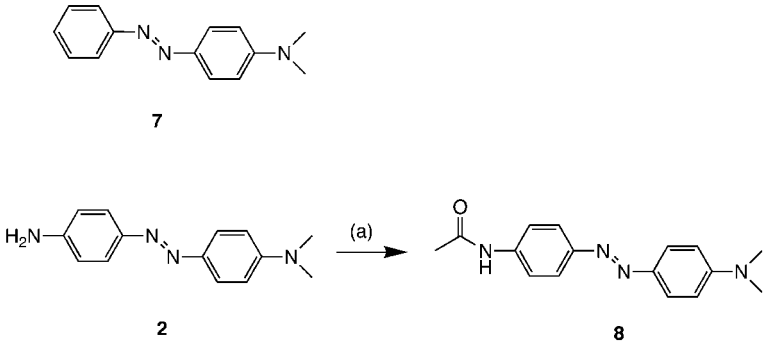

Scheme 3. 4-DMAzo derivatives: 4-DMAzo **7**, 4′-amino-4-DMAzo **2**, and 4′-acetoamide-4-DMAzo **8**. (a) Acetyl chloride, triethylamine, CH_2Cl_2, 85% yield.

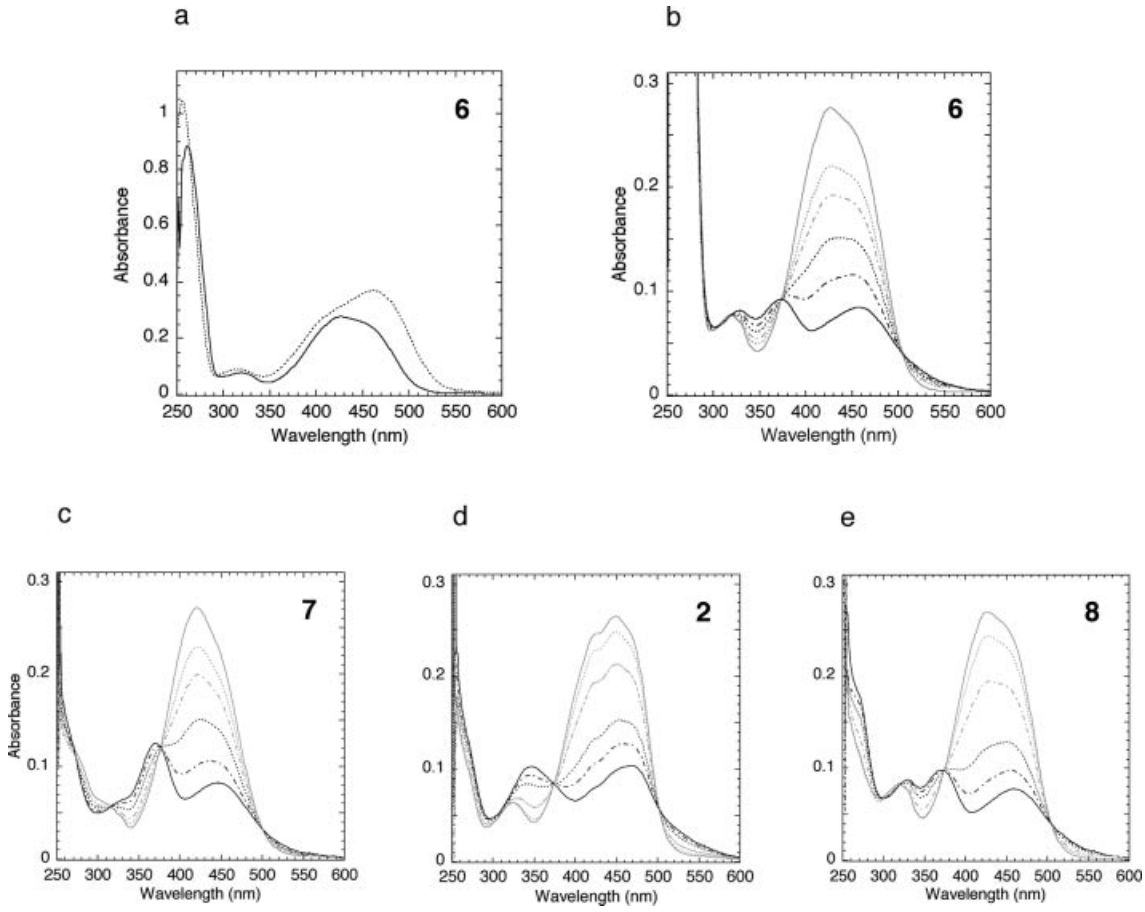

Figure 1. Photoresponsive spectral profiles of the oligonucleotide **6** and 4-DMAzo derivatives (**2**, **7**, and **8**). (a) Spectral profiles of **6** in DMSO (7.1 μM; solid line) and in water containing ammonium formate (50 mM) (9.2 μM; dotted line) before irradiation with visible (420 nm) light. (b–d) Time course of the spectral changes of the 4-DMAzo moiety in **6** and 4-DMAzo derivatives in DMSO at controlled temperature (20.0 ± 0.1 °C) after irradiation with 420 nm light, corresponding to thermal (*Z*)-to-(*E*) transition. (b) Spectral profiles of **6** (7.1 μM) in the visible region are shown (with rising absorbance at ca. 400 nm in the visible region) 0, 10, 30, 60, and 90 min after and before irradiation, respectively. (c) 4-DMAzo **7** (8.7 μM, with rising absorbance at ca. 400 nm) at 0, 90, 270, 540, and 810 min after and before irradiation, respectively. (d) 4′-Amino-4-DMAzo **2** (7.1 μM, with rising absorbance at ca. 400 nm) at 0, 1, 3, 10, and 20 min after and before irradiation, respectively. (e) 4′-Acetamido-4-DMAzo **8** (8.0 μM, with rising absorbance at ca. 400 nm) at 0, 10, 30, 90, and 180 min after and before irradiation, respectively.

Photoresponsivity of 6 to Visible Light in DMSO

As mentioned in the Introduction, no (*E*)/(*Z*) transitions in aqueous solutions had been detected in oligonucleotides bearing azobenzene derivatives with dimethylamino groups at their 4-positions.[11,13] We speculated that, in aqueous solutions, the dimethylamino group of the 4-DMAzo moiety in **6** undergoes protonation, similarly to the parent 4-DMAzo or 4′-carboxy-4-DMAzo,[18] so that no significant spectral change in **6** is detectable with a conventional spectrophotometer due to the rapid thermal (*Z*)-to-(*E*) transition. For this reason we attempted to observe changes in the absorption spectra with a conventional spectrophotometer by conducting measurements in DMSO, an aprotic solvent that should suppress protonation of the dimethylamino group. Figure 1 (b) shows spectral changes of **6** before and after visible-light (λ = 420 nm) irradiation in DMSO that had been thoroughly dried to avoid protonation from water molecules. The two spectra were significantly different, corresponding to the (*E*) form [gray solid line in Figure 1 (b)] and the (*Z*) form, which has clearly distinguishable n–π* and π–π* bands [black solid line in Figure 1 (b)]. Clear isosbestic points at $\lambda \approx$ 317, 374, and 505 nm were obtained by tracing the spectra during thermal recovery isomerization [Figure 1 (b)]. Figure 1 (c–e) shows the significant spectral changes seen in the 4-DMAzo derivatives **7**, **2**, and **8**, respectively, upon visible-light irradiation [(*E*) and (*Z*) forms shown in solid gray and black lines, respectively]. The spectral profile and isosbestic points of **6** incorporating the (*Z*) form of 4-DMAzo are similar to those of the (*Z*) form of **8** [isosbestic points at $\lambda \approx$ 320, 374, and 505 nm in **8**, as determined from Figure 1 (e)]. This result is consistent with the similarity of the (*E*) forms of **6** and **8**, as described above.

The rate constants ($k_{(Z)-(E)}$) of thermal (*Z*)-to-(*E*) isomerization of **6** and of the 4-DMAzo derivatives (**2**, **7**, and **8**) in DMSO were estimated by first-order kinetic analysis of the time courses of spectral changes in the recovery transitions of these compounds as shown in Figure 1 (b–e)

(Table 2). The $k_{(Z)-(E)}$ value of **6** was larger than that of **7**, smaller than that of **2**, and similar to that of **8**. It is known that the rates of thermal (*Z*)-to-(*E*) isomerization of *para*-donor/*para*′-acceptor-substituted ("push-pull-substituted") azobenzenes such as 4′-nitro-4-DMAzo and "push-push"-substituted azobenzenes such as 4′-(dialkylamino)-4-DMAzo compounds are faster than that of 4-DMAzo.[19,20] The electron transition state of **2** should be most similar to those of "push-push" azobenzenes, consistent with the finding that the rate for **2** was the largest of all four compounds examined in this experiment. The $k_{(Z)-(E)}$ values of **6** and **8** were significantly smaller than that of **2**, suggesting that the amide bonds and attached DNA or the methyl group at the 4′-positions are poor donors or acceptors relative to the 4′-amino group in **2**, not to mention the 4′-nitro or 4′-(dialkylamino) groups. The $k_{(Z)-(E)}$ value for **6**, as well as its spectral properties, were similar to those of **8**, indicating that the optical properties of **6** are similar to those of **8**. Nonetheless, the $k_{(Z)-(E)}$ value for **6** is slightly larger than that for **8**, implying that protons of the DNA backbone affect the rate of thermal (*Z*)-to-(*E*) isomerization to some extent.

Table 2. Rate constants ($10^2 k_{(Z)-(E)}$ min^{-1}; average ± s.d.) for thermal (*Z*)-to-(*E*) isomerization of the 4-DMAzo derivatives (**2**, **7**, and **8**) and the photoresponsive oligonucleotide **6** in DMSO at 20.0 ± 0.1 °C.

Compound	**7**	**2**	**8**	**6**
$10^2 k_{(Z)-(E)}$	0.224 ± 0.033	12.4 ± 0.20	1.13 ± 0.01	1.54 ± 0.19

Photoinduced Reversible Isomerization of 6 in DMSO

Figure 2 shows the photoinduced reversible spectral changes of **6** in DMSO. A proportion of 4-DMAzo tethered in **6** underwent (*E*)-to-(*Z*) isomerization upon irradiation with 420 nm light (from the gray solid line to the gray dotted line in Figure 2, top), followed by photoinduced (*Z*)-to-(*E*) recovery upon 7 min of irradiation with 550 nm light in the visible region (from the gray dotted line to the black solid line in Figure 2, top) or with 350 nm light in the UV region (from the gray dotted line to the black dotted line in Figure 2, top). The extent of thermal (*Z*)-to-(*E*) recovery in 7 min (from the gray dotted line to the gray dashed-dotted line in Figure 2, top) corresponded to ca. 20% of the total conversion induced by 7 min of irradiation with visible or UV light. The photoresponsive properties of **6** were distinct from those of the parent azobenzene-conjugated oligonucleotide, in which the (*E*)-to-(*Z*) isomerization is triggered by UV light and the (*Z*)-to-(*E*) isomerization is triggered only by visible light.[6] The extent of reversible isomerization had not decayed after 10 cycles of alternate irradiation with 420 nm and either 550 nm or 350 nm light (Figure 2, bottom). The absorbance at 425 nm decreased to ca. 26% at the photostationary state (rectangles in Figure 2, bottom) and recovered to ca. 80% (circles and triangles in Figure 2, bottom) of that of the pure (*E*) state (the initial point at 0 cycles in Figure 2, bottom) on irradiation with 420 nm light and either 350 nm or 550 nm light (each absorbance value is the average of 10 cycles).

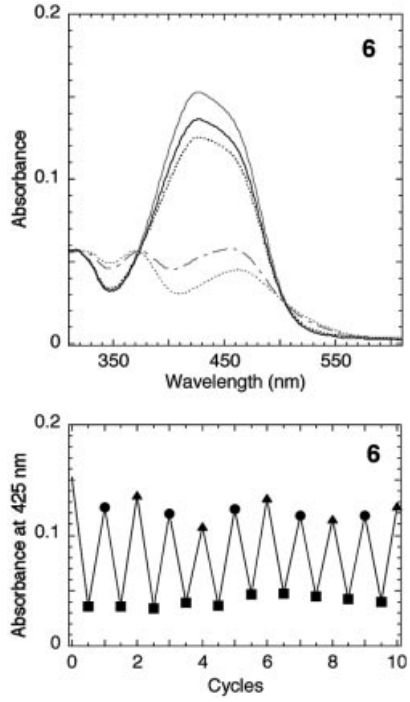

Figure 2. Photoinduced reversible isomerization of **6** (3.9 μM) in DMSO. Top: Spectral changes of the 4-DMAzo moiety in **6** before (gray solid line) and after (gray dotted line) irradiation with 420 nm light, followed by irradiation either with visible (λ = 550 nm) light (black solid line) or with UV (λ = 350 nm) light (black dotted line). Thermal recovery that had occurred after 7 min in the dark is shown by the gray dashed-dotted line. Bottom: The cycles of alternating reversible changes in absorbance at λ = 425 nm for (*E*)-to-(*Z*) isomerization upon 420 nm irradiation (squares), followed by (*Z*)-to-(*E*) photoinduced isomerization upon irradiation either with 550 nm (circles) or with 350 nm (triangles) light. The sample was irradiated for 7 min in a fluorescence spectrophotometer immediately before each measurement at 20.5 ± 1 °C.

Detection of the Photoresponsivity of 6 to Visible Light in Aqueous Solution

With a conventional spectrophotometer we were unable to detect changes in the spectral profile of **6** in an aqueous solution after irradiation with visible light (420 nm) [Figure 3 (a), solid and dotted lines], consistent with previous reports,[11,13] so we attempted to detect (*E*)/(*Z*) isomerization by laser flash photolysis.[17] Figure 3 (b) shows the changes in absorbance at 460 nm after a laser (λ = 532 nm) photoflash. Upon triggering of the flash, which lasted for 3–5 ns (arrow), the absorbance decreased instantly, indicating photoinduced (*E*)-to-(*Z*) isomerization. This absorbance decrease was followed by recovery within ca. 1 ms, representing rapid (*Z*)-to-(*E*) thermal isomerization [Figure 3 (b), dark gray line]. Fitting to a first-order exponential equation yielded a time constant of 0.14 ± 0.01 ms (average ± s.d., n = 3) [Figure 3 (b), solid black curve], or a

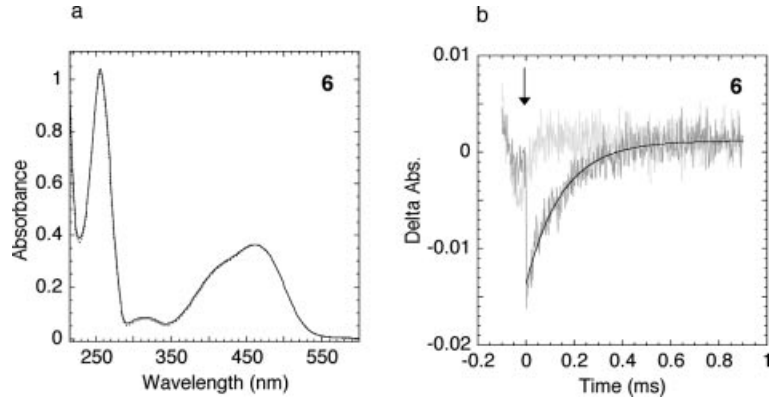

Figure 3. Photoresponsivity of **6** in an aqueous solution (50 mM ammonium formate) at room temperature. The concentration of **6** was 9.2 μM, as estimated from the absorbance at 260 nm. (a) Absorbance spectra of **6** observed with a conventional spectrophotometer before (solid line) and after (dotted line) irradiation with visible light (420 nm) for 30 min. (b) Profiles of absorbance changes at 460 nm in **6** after a laser photoflash (arrow, λ = 532 nm). The traces shown in dark and pale gray are the profiles obtained for **6** and for a control 8-mer adenosine oligonucleotide (normalized), respectively. The solid black line is the fit with a first-order exponential equation [$y = a\cdot\{1 - \exp(-t/b)\} + c$; t = time (ms); fitting parameters: a = 0.015, b = 0.15, c = 0.014; R = 0.95].

rate constant of $k_{(Z)-(E)} \approx 4.3 \times 10^5$ min^{-1}. The contribution made to the exponential recovery by diffusion was negligible, because the detection area ($\phi \approx 1$ mm) was much larger than the diffusion field covered by **6** in 1 ms.

As described above, the electron transition state of **6** is distinct from those of the "push-push" or "push-pull" azobenzene derivatives because the rate of thermal (*Z*)-to-(*E*) isomerization of **6** in DMSO is significantly smaller than those of "push-push" or "push-pull" compounds (for instance, $k_{(Z)-(E)} = 7.2 \times 10^3$ min^{-1} for 4′-nitro-4-DMAzo in DMSO,[19] in comparison to ca. 1.5×10^{-2} min^{-1} for **6**). We therefore speculate that the rapid thermal (*Z*)-to-(*E*) isomerization of **6** in aqueous solutions is mostly due to protonation by water molecules rather than the high polarity of the solvent.

Conclusions

We have demonstrated substantial optical responsivity of an oligonucleotide incorporating a 4-DMAzo unit – an azobenzene derivatized with a dimethylamino group – to irradiation with visible light. We are now able to regulate the structural changes of a 4-DMAzo moiety in a photoresponsive oligonucleotide both in aqueous solutions and in aprotic solvents such as DMSO. Although thermal (*Z*)-to-(*E*) recovery in aqueous solution was too rapid to allow light-induced (*Z*)-to-(*E*) recovery in this study, it might in theory be possible to restrain a controlled proportion of 4-DMAzo moieties in the (*Z*) form in aqueous solutions by continuous irradiation with visible light. With regard to the use of 4-DMAzo moieties tethered to oligonucleotides in aprotic solvents, it is known that the secondary structure of double-stranded DNA is unstable in DMSO, so the assembly of DNA-based devices driven by photoregulated hybridization involving 4-DMAzo in organic solvents would require developments of aprotic solvents that would allow the formation of stable double helixes, such as that demonstrated by Okahata et al.[21] Efforts in that direction are currently underway.

Availability of pseudo-nucleotides bearing different azobenzene derivatives or other photochromic molecules, as well as different methods of incorporating the photochromic systems into the nucleotides, should expand the repertoire of optical properties of photoresponsive oligonucleotides.[5,22,23] This should in turn facilitate the development of a variety of photoregulated and photoprogrammable DNA nanodevices.

Experimental Section

General: All solvents and reagents except for DMSO were obtained from commercial sources and were used for syntheses and spectroscopic measurements without further purification. DMSO (Tokyo Kasei) was used after drying with ca. 1/3 of its volume of molecular sieves (Wako). Thin-layer chromatography (TLC) was performed on silica gel pre-coated onto an aluminium sheet (silica gel 60 F254, Merck). The silica gel used for flash column chromatography was purchased from Kanto Chemical (silica gel 60N, spherical, neutral, 40–50 μm). The paper filters used for filtration were purchased from Kiriyama (Nos. 5B or 5C). For identification of the synthesized products, ^{1}H NMR spectra were measured with a Gemini-2000/300BB (300 MHz) (Varian).

4′-Amino-4-DMAzo (2): A mixture of *N*,*N*-dimethyl-*p*-nitrosoaniline (Wako, 0.920 g, 6.1 mmol) and *p*-phenylenediamine (Wako, 0.661 g, 6.1 mmol) in benzene (60 mL) containing glacial acetic acid (0.5 mL) was heated at reflux under a Dean–Stark trap at 85 °C for more than 24 h. The reaction mixture was allowed to cool to room temperature, filtered, and concentrated to provide the crude product, which was purified by flash column chromatography on silica gel (0.61 g, 41.5% yield). ^{1}H NMR [$CDCl_3$ (TMS)]: δ = 7.82–6.71 (m, 8 H, aromatic protons of azobenzene), 3.91 (s, 2 H, NH_2), 3.06 [s, 6 H, N(CH_3)$_2$] ppm. R_f = 0.17 (CH_2Cl_2).

***N*-(4-{[4-(Dimethylamino)phenyl]azo}phenyl)-3-hydroxy-2-(hydroxymethyl)-2-methylpropionamide (3):** In dry DMF (12.5 mL), 2,2-bis(hydroxymethyl)propionic acid (Sigma–Aldrich, 2.09 g, 15.6 mmol), 4′-amino-4-DMAzo (3.12 g, 13.0 mmol), anhydrous 1-

hydroxybenzotriazole (HOBt, Dojindo, 2.11 g, 15.6 mmol), and dicyclohexylcarbodiimide (Sigma–Aldrich, 3.21 g, 15.6 mmol) were stirred under nitrogen at room temperature overnight (ca. 16 h) and then at 100 °C for 4 h. Then, ethyl acetate (225 mL) was added, and the ethyl acetate solution was filtered and washed once each with 225 mL of saturated aqueous solutions of $NaHCO_3$ and NaCl. The organic layer was dried with anhydrous Na_2SO_4, filtered, and concentrated, and the crude product was dried in vacuo and purified by silica gel flash column chromatography (CH_2Cl_2/MeOH, 95:5) to provide 1.23 g (26.6% yield). ^{1}H NMR [300 MHz, $CDCl_3$(TMS)]: δ = 9.22 (s, 1 H, N*H*CO), 7.88–6.74 (m, 8 H, aromatic protons of azobenzene), 3.91–3.87 (m, 4 H, CH_2), 3.09 [s, 6 H, N(CH_3)$_2$], 2.81 (m, 2 H, O*H*), 1.23 (s, 3 H, CH_3) ppm. R_f = 0.26 (CH_2Cl_2/MeOH, 95:5). ESI MS: *m*/*z* = 357.2 [M + H]$^+$ (calcd. 357.2).

3-[Bis(4-methoxyphenyl)(phenyl)methoxy]-*N*-{4-[(4-dimethylamino)-phenylazo]phenyl}-2-(hydroxymethyl)-2-methylpropionamide (4): A dry pyridine (15 mL) solution of **3** (1.97 g, 5.53 mmol) and 4-(dimethylamino)pyridine (DMAP, Tokyo Kasei, 5.66 mg, 0.276 mmol) was cooled under nitrogen with ice, and 4,4′-dimethoxytrityl chloride (DMT-Cl, Wako, 2.25 g, 6.63 mmol) in CH_2Cl_2 (4.5 mL) was added dropwise. After 19 h, CH_2Cl_2 (60 mL) was poured into the mixture, and the solution was filtered. After having been washed with saturated aqueous solutions (60 mL) of $NaHCO_3$ (twice) and NaCl (once), the organic layer was dried with anhydrous Na_2SO_4, the solution was concentrated and dried in vacuo, and silica gel column chromatography (CH_2Cl_2/*i*PrOH/Et_3N, 97.5:2.5:1) provided **4** (1.93 g, 53.0% yield). ^{1}H NMR [300 MHz, $CDCl_3$(TMS)]: δ = 9.45 (s, 1 H, N*H*CO), 7.87–6.74 (m, 21 H, aromatic protons of azobenzene and DMT), 3.79–3.64 (s, 6 H, OCH_3, m, 2 H, CH_2OH), 3.44–3.36 (d, 2 H, DMT-OCH_2), 3.07 [s, 6 H, N(CH_3)$_2$] 1.35 (s, 3 H, CH_3) ppm. R_f = 0.25 (CH_2Cl_2/*i*PrOH/Et_3N, 97.5:2.5:1). ESI MS: *m*/*z* = 659.3 [M + H]$^+$ (calcd. 659.3).

2-{[Bis(4-methoxyphenyl)(phenyl)methoxy]methyl}-3-(4-{[4-(dimethylamino)phenyl]azo}phenylamino)-2-methyl-3-oxopropyl 2-Cyanoethyl diisopropylphosphoramidite (5): In a dry acetonitrile (10 mL) solution, **2** (0.296 g, 0.45 mmol) and 2-cyanoethyl *N*,*N*,*N*′,*N*′-tetraisopropylphosphorodiamidite (Sigma–Aldrich, 0.16 mL, 0.50 mmol) were treated with 1*H*-tetrazole (Tokyo Kasei, 35 mg, 0.50 mmol). After 1 h, the product was added to ethyl acetate (100 mL), and the organic solution was filtered and washed with 100 mL portions of saturated aqueous solutions of $NaHCO_3$ and NaCl, dried with Na_2SO_4, and desalted by filtration. Finally, the solvent was removed in vacuo. The resultant product was purified by silica gel column chromatography (hexane/AcOEt, 2:1) and dried in vacuo to provide 0.14 g (36.2% yield). ^{1}H NMR [300 MHz, $CDCl_3$(TMS)]: δ = 9.16 (s, 1 H, N*H*CO), 7.86–6.74 (m, 21 H, aromatic protons of azobenzene and DMT), 3.85–3.71 (m, 10 H, OCH_3, CH_2OP, CH_2-OP), 3.54–3.46 [m, 2 H, C*H*(CH$_3$)$_2$], 3.42–3.37 (m, 2 H, DMT-OCH_2), 3.08 [s, 6 H, N(CH_3)$_2$], 2.56–2.47 (m, 2 H, CH_2CN), 1.28–1.07 [m, 15 H, CH(CH_3)$_2$, CH_3] ppm. R_f = 0.28 (hexane/AcOEt, 2:1). ESI MS: *m*/*z* = 881.5 [M + Na]$^+$ (calcd. 881.4).

Synthesis of Photoresponsive Oligonucleotide 6: To prepare the photoresponsive DNA oligonucleotide with an automated synthesizer (DNA/RNA synthesizer 392/394, ABI), the phosphoramidite monomer **5** was diluted to 0.1 M in dry acetonitrile. Monomer **5** was coupled with a conventional adenine-phosphoramidite monomer to synthesize the photoresponsive oligonucleotide on a 0.2 μmol scale. The synthesized oligonucleotide was adsorbed on a CPG column (500 Å pore size) and eluted by ammonia treatment for cleavage. The resultant crude product for HPLC purification was obtained after incubation at 55 °C for 12 h and freeze-drying. All reagents for the synthesis of the oligonucleotide were purchased from ABI, except for ammonia solution (WAKO).

***N*-(4-{[4-(Dimethylamino)phenyl]azo}phenyl)acetamide (8):** Compound **2** (0.10 g, 0.42 mmol) in CH_2Cl_2 (1.4 mL) and triethylamine (0.1 mL) solution was added dropwise under nitrogen to acetyl chloride (33 mg, 0.42 mmol, WAKO) prepared as a CH_2Cl_2 solution (6% v/v, 0.8 mL). The product was added to CH_2Cl_2 (20 mL), the solution was filtered, and the organic layer was washed with saturated aqueous solutions (20 mL) of $NaHCO_3$ (twice) and NaCl (twice) and then dried with anhydrous Na_2SO_4. The solution was concentrated and dried in vacuo. Silica gel column chromatography (CH_2Cl_2/MeOH, 95:5) provided **8** (0.10 g, 85% yield). ^{1}H NMR [300 MHz, [D$_6$]DMSO (TMS)]: δ = 10.17 (s, 1 H, N*H*CO), 7.77–6.81 (m, 8 H, aromatic protons of azobenzene), 3.08 [s, 6 H, N(CH_3)$_2$], 2.08 (s, 3 H, CH_3) ppm. R_f = 0.44 (CH_2Cl_2/MeOH, 95:5).

Reversed-Phase HPLC Purification of 6: The sample solution was filtered (Millex, 0.45 μm, Millipore) before application to the column (Symmetry C18, 5 μm, 100 Å, Waters) for reversed-phase HPLC purification (JASCO). The developing solvent flowed for 50 min at a rate of 1 mL min^{-1} and was composed of a linear gradient from 5:95% to 45:55% acetonitrile/water (50 mM ammonium formate) at room temperature. The first major peak was observed at ca. 17 min, and the second peak was observed ca. 40 s later after correction for the dead volume. The monitoring wavelength was 260 nm. The results reported in this paper were obtained by use of the fraction with the longer retention time, although two distinct spectral profiles corresponding to the (*E*) and (*Z*) forms of 4-DMAzo-tethered **6** were also observed in DMSO with the fraction of shorter retention time. Furthermore, the time constant for recovery in aqueous solution after flash photolysis was 0.14 ± 0.1 ms for the fraction with the shorter retention time, similar to that obtained for that with the longer retention time.

ESI and MALDI-TOF Mass Measurements: Compounds **3**–**5** were identified by NMR spectroscopy and ESI mass spectrometry (positive mode, MeOH solvent; ABI). The synthesized oligonucleotide **6** was identified by MALDI-TOF mass spectrometry (negative mode, THAP matrix; ABI).

UV/Vis Spectroscopy: Spectra of the synthesized oligonucleotide, 4-DMAzo and its derivatives were measured with a DU800 spectrophotometer (Beckman). Prior to the (*Z*)/(*E*) transition measurements with the spectrophotometer, the sample solutions were irradiated with light. The sample cell (quartz) was irradiated with UV (350 nm) or visible (420 or 550 nm) light from a 150 W Xenon lamp through a 5 nm slit for 25 min or longer at 20.5 ± 1 °C by placing a quartz cuvette containing the sample in the light path of a fluorescence spectrometer (RF-5300PC, Shimadzu). Before each experiment we confirmed that the absorbance of the sample at 425 nm did not change over a 15–30 min period in the dark; this is an indication that the majority of the 4-DMAzo moieties were originally in the (*E*) form, as was also confirmed by NMR analysis of **8** (data not shown). All procedures were performed in a dark room.

Kinetic Measurement in DMSO: The rate constants of thermal (*Z*)-to-(*E*) isomerization were estimated by first-order analysis of the absorbance at λ = 425 nm for at least three measurements. The *R* values were >0.99 for all compounds. The mixtures of solute (**6** or the 4-DMAzo derivatives) and DMSO were dried thoroughly by incubation with molecular sieves for more than 8 h before each measurement in a dark place. The concentration of each compound was as follows: **6** (3.9–8.3 μM), **2** (7.1–8.7 μM), **7** (8.3–8.7 μM), and

8 (8.0–10 μM). The concentration of **6** was estimated from the absorbance at λ_{max} in DMSO, which was calibrated from the absorbance in aqueous solution at 260 nm. Concentrations of **2**, **7**, and **8** were estimated by using ε = 37300, 31200, and 33900 M^{-1}, respectively, determined from the weight and molecular weight. These values are in good agreement with predicted values for 4-DMAzo derivatives from a previous report.[19] Preliminary NMR and spectral analyses suggested that the fractions of 4-DMAzo moieties that had undergone (*E*)-to-(*Z*) isomerization after irradiation with 420 nm light were at least 74%, 74%, 63%, and 78% in **6**, **2**, **7**, and **8** (data not shown). Fractions of 4-DMAzo moieties that had undergone thermal recovery to the (*E*) forms during preparation of measurements and wavelength scanning, as estimated from the rate constants, were 1.2% (**6**), 6.7% (**2**), 0.18% (**7**), and 1.1% (**8**).

Laser Flash Photolysis: The flash photolysis experiment was performed with a Minilite II instrument (Unisoku) at room temperature. The sample solution was irradiated in a cuvette ($10 \times 10 \times 16$ mm) at λ = 532 nm with a laser (average power 375 mW; pulse width 3–5 ns). The beam size was ca. 3 mm and was expanded to ca. 3×10 mm through a cylindrical lens. The monitoring light (460 nm, ϕ = 1 mm) was orthogonal to the excitation light and was detected on the other side of the cuvette. Traces after 30 flashes made at 1 s intervals were integrated, and the rate constants for thermal (*Z*)-to-(*E*) isomerization were obtained by first-order kinetic analysis of the traces. The control oligonucleotide, 5′-AAAAAAAA-3′ (HPLC-purification grade), was purchased from Hokkaido System Science.

Acknowledgments

This work was supported by the AIST Upbringing of Talent in Nanobiotechnology Course, Promotion Budget for Science and Technology, from the Ministry of Education, Culture, Sports, and Technology of Japan.

[1] K. Ichimura, S. K. Oh, M. Nakagawa, *Science* **2000**, *288*, 1624–1626.
[2] K. Kinbara, T. Aida, *Chem. Rev.* **2005**, *105*, 1377–1400.
[3] T. Muraoka, K. Kinbara, T. Aida, *Nature* **2006**, *440*, 512–515.
[4] Y. Norikane, N. Tamaoki, *Org. Lett.* **2004**, *6*, 2595–2598.
[5] K. Yamana, A. Yoshikawa, H. Nakano, *Tetrahedron Lett.* **1996**, *37*, 637–640.
[6] H. Asanuma, T. Ito, M. Komiyama, *Tetrahedron Lett.* **1998**, *39*, 9015–9018.
[7] H. Asanuma, T. Ito, T. Yoshida, X. G. Liang, M. Komiyama, *Angew. Chem. Int. Ed.* **1999**, *38*, 2393–2395.
[8] K. Takahashi, S. Yaegashi, H. Asanuma, M. Hagiya, *DNA Computing* **2006**, *3892*, 336–346.
[9] H. Asanuma, K. Shirasuka, M. Komiyama, *Chem. Lett.* **2002**, 490–491.
[10] H. Asanuma, K. Shirasuka, T. Takarada, H. Kashida, M. Komiyama, *J. Am. Chem. Soc.* **2003**, *125*, 2217–2223.
[11] T. Gunnlaugsson, J. M. Kelly, M. Nieuwenhuyzen, A. M. K. O'Brien, *Tetrahedron Lett.* **2003**, *44*, 8571–8575.
[12] M. Kubota, A. Ono, *Tetrahedron Lett.* **2004**, *45*, 5755–5758.
[13] H. Kashida, M. Tanaka, S. Baba, T. Sakamoto, G. Kawai, H. Asanuma, M. Komiyama, *Chem. Eur. J.* **2006**, *12*, 777–784.
[14] M. E. Neubert, S. J. Hummel, J. C. Bhatt, S. S. Keast, A. M. Lackner, J. D. Margerum, E. Sherman, *Mol. Cryst. Liq. Cryst.* **1995**, *260*, 287–300.
[15] M. Endo, Y. Azuma, Y. Saga, A. Kuzuya, G. Kawai, M. Komiyama, *J. Org. Chem.* **1997**, *62*, 846–852.
[16] X. G. Liang, H. Asanuma, H. Kashida, A. Takasu, T. Sakamoto, G. Kawai, M. Komiyama, *J. Am. Chem. Soc.* **2003**, *125*, 16408–16415.
[17] P. D. Wildes, G. J. Pacifici, G. J. Irick, D. G. Whitten, *J. Am. Chem. Soc.* **1971**, *93*, 2004–2008.
[18] A. Sanchez, R. H. Derossi, *J. Org. Chem.* **1993**, *58*, 2094–2096.
[19] N. Nishimura, T. Sueyoshi, H. Yamanaka, E. Imai, S. Yamamoto, S. Hasegawa, *Bull. Chem. Soc. Jpn.* **1976**, *49*, 1381–1387.
[20] N. Nishimura, T. Tanaka, M. Asano, Y. Sueishi, *J. Chem. Soc., Perkin Trans. 2* **1986**, 1839–1845.
[21] Y. Okahata, K. Ijiro, Y. Matsuzaki, *Langmuir* **1993**, *9*, 19–21.
[22] K. Yamana, A. Yoshikawa, R. Noda, H. Nakano, *Nucleosides Nucleotides* **1998**, *17*, 233–242.
[23] R. L. Letsinger, T. F. Wu, *J. Am. Chem. Soc.* **1994**, *116*, 811–812.

Received: October 26, 2006
Published Online: February 23, 2007

